JOURNAL OF MATERIALS SCIENCE 22 (1987) 4077–4086

# Effect of porosity and alumina content on the high temperature mechanical properties of compocast aluminium alloy–alumina particulate composite

P. K. GHOSH, S. RAY
*Department of Metallurgical Engineering, University of Roorkee, Roorkee – 247667, India*

The effects of volume fraction of alumina and porosity on the tensile strength of Al–4 wt% Mg–alumina compocast particulate composite tested at various temperatures up to 623 K have been investigated with the help of a phenomenological model. The contribution of porosity on reduction of strength of composites at various levels of alumina content has been expressed as a linear function of porosity and the resulting equation contains two experimentally determined parameters, $\sigma_0$, the ultimate tensile strength at zero porosity level and $\alpha$, a weakening factor. It is observed that $\alpha$ decreases with an increase in volume fraction of alumina in the composite and it becomes more sensitive to alumina content of the composite with a rise in temperature. At a given alumina content $\alpha$ increases with a rise in test temperature but this effect is gradually countered by increasing alumina content of the composite. Finally, in a composite having ~10.3 vol% alumina $\alpha$ decreases with an increase in temperature. This may have occurred because the extent of particle–matrix debonding is determined by the plastic strain in the matrix and the fracture strain of a composite increases or decreases with temperature when the alumina content lies below or above ~9.0 vol% of alumina respectively. At any test temperature $\sigma_0$ of the composite decreases rapidly with an increase in volume fraction of alumina, but the rate of decrease of $\sigma_0$ reduces at higher alumina levels. However at the elevated temperatures of 473 K and 573 K a sharp fall in $\sigma_0$ is observed at alumina contents beyond ~9.0 vol%. At a lower level of alumina content below about 8.98 vol% the fracture strain of the composites increases with an increase in temperature. However, in the case of higher alumina content beyond the level mentioned above the fracture strain of the composites decreases with the rise in temperature. At a given porosity level the fracture strain of a composite having about 9.4 vol% alumina decreases with an increase in temperature. Scanning electron microscopic observations show that the extent of the growth and linkage of voids before fracture become extensive at higher temperature. At ambient temperature the composites fail by a mixed mode of ductile and clevage fracture. At 573 K a number of considerably small dimples along with the larger ones are observed in the fractured surface. At this temperature a large number of newly formed fine grains are observed in the matrix.

## 1. Introduction

The volume fraction of porosity and reinforcing particles along with their shape, size and distribution in a compocast particulate composite play an important role in controlling its mechanical properties. The amount, shape, size and distribution of particles can be regulated by choosing suitable particles and casting process parameters [1] but a control of porosity is difficult. The mechanical properties of compocast aluminium alloy–alumina composites have been correlated to the volume fraction of porosity content [2]. Using a phenomenological model the contribution of porosity in reducing the room temperature tensile strengths of composites containing different level of alumina particles have been estimated and the projected strength at zero porosity level have been determined [3].

In the present investigation the effect of volume fraction of particles on the tensile strength in a compocast composite containing alumina particles dispersed in Al–4 wt % Mg alloy have been studied at elevated temperatures. The role of porosity in reducing the elevated temperature strength of a composite at given levels of alumina content have been determined at different temperatures to project the ultimate tensile strength at zero porosity level.

## 2. Experimental procedure

An alumina–aluminium–magnesium alloy particulate composite was prepared by melting about 500 g of

0022–2461/87 $03.00 + .12 

TABLE I Distribution of various sizes of particles in the alumina powder used

| Size distribution | Size of the alumina particles ($\mu$m) | | | | | | | | |
|---|---|---|---|---|---|---|---|---|---|
| | +212 | +180, −212 | +125, −180 | +106, −125 | +75, −106 | +63, −75 | +53, −63 | +45, −53 | −45 |
| Amount (wt %) | 0.31 | 49.37 | 13.90 | 31.56 | 1.87 | 1.73 | 0.33 | 0.15 | 0.78 |

aluminium of commercial purity in a graphite crucible placed in a resistance heating furnace having an arrangement for bottom pouring. A magnesium lump weighing about 25 g was added to the melt. The melt was vigorously stirred mechanically with an impeller at different speeds in the range of 400 to 1500 r.p.m. During stirring the melt was allowed to cool through the solidification range of the alloy till the desired pouring temperature was attained. Alumina particles with a broad spectrum of sizes as mentioned in Table I, preheated to 1072 K was added to the vortex formed on the melt surface while stirring at the pouring temperature of 900 K which lies in the semisolid region of the alloy. After addition of the particles the slurry was continously stirred for 225 to 240 sec during which the temperature of the slurry was maintained to within $\pm 5$ K of the pouring temperature. Then the slurry was poured into a 25 mm × 30 mm × 300 mm steel mould through the bottom of the crucible by removing the graphite stopper and the ingot was immediately cooled by spraying with water. The chemical analysis of the Al–Mg alloy matrix showed that it contained 4.0% Mg, 0.98% Fe, 0.3% Si, 0.05% Mn, 0.01% Ti and the balance of aluminium.

Suitable metallographic specimens were taken from the adjoining regions of the castings used for fabrication of tensile specimens and were prepared using standard metallographic procedures. The specimens were observed under an optical microscope for the estimation of the extent of incorporation of alumina particles and the porosity content of the composite. The particle–matrix interface was examined with a scanning electron microscope.

The tensile specimens of dimensions as given in Fig. 1 was machined out from the pieces of different castings. The volume fraction of alumina particles and porosity in each tensile specimen were determined by point counting under an optical microscope and the observed density of each tensile specimen [1]. Tensile tests were carried out on a Hounsfield Tensometer at an ambient temperature of 298 K and at high temperatures between 373 K and 623 K. In the high temperature tests the specimens were soaked for 700 to 750 sec at the test temperature inside a resistance heating tube furnace and then fractured under tension inside the furnace. The temperature of the furnace was measured using a chromel–alumel thermocouple just by the side of the specimen inside the furnace. During soaking and testing the temperature of the furnace was maintained to within $\pm 4$ K. The fractured surfaces of the specimens tested at different temperatures were examined with a scanning electron microscope. The longitudinal sections of the specimens tested under tension were polished and prepared for a study of the change in microstructures in the specimens resulting during mechanical testing at high temperature.

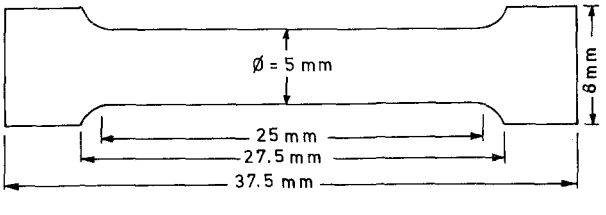


*Figure 1* Schematic diagram of the tensile specimen.

## 3. Results

A typical distribution of alumina particles in the composite having about 12.5 vol % particle is shown in Fig. 2. The interface of reinforcing alumina particles with the matrix as observed under a scanning electron microscope is shown in Fig. 3. The micrograph shows that a reacted layer has formed at the interface.

For samples containing a definite amount of alumina particles, the ultimate tensile strength $\sigma_p$, at different vol % of porosity, $P$, have been determined at different temperatures. A linear behaviour of $\sigma_p$ with $P$ at ambient temperature (298 K) has been derived phenomenologically for low porosity content and in this class of material this linear relation has been amply justified experimentally. It has been proposed that

$$\sigma_p/\sigma_0 = 1 - \alpha P \quad (1)$$

when, $\sigma_0$ is the projected ultimate tensile strength of the composite at zero porosity for a given alumina content and $\alpha$ is called the weakening factor. For composites having low alumina contents in the range

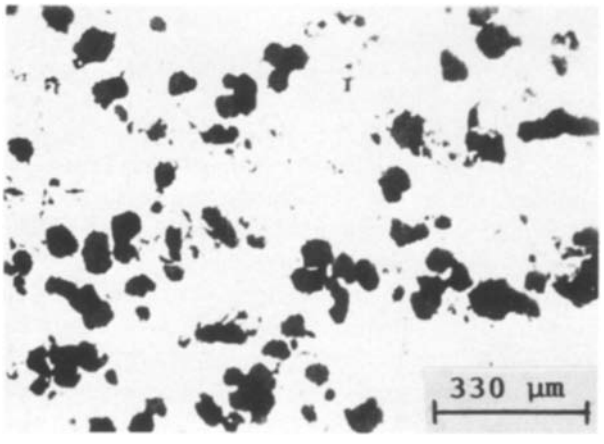


*Figure 2* A typical distribution of alumina particles in the composite.

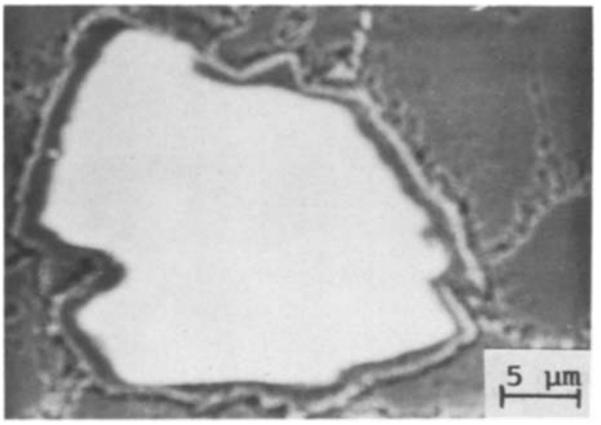


*Figure 3* Scanning electron micrograph showing a reacted layer at the particle–matrix interface.

of 2.0 to 2.6 vol % and tested at temperatures of 298, 473 and 573 K, the typical variations of $\sigma_p/\sigma_0$ with $P$ have been shown in Fig. 4. The same behaviour for composites having higher alumina contents of 9.2 and 10.5 vol % and tested at 473 and 573 K have also been shown in Fig. 4. The figure shows that even at elevated temperatures the tensile strength of these composites are linear functions of porosity content. The effect of alumina content of the composite on $\alpha$ at ambient and elevated temperatures of 298, 473 and 573 K are shown in Fig. 5. The values of $\alpha$ have been found to decrease with an increase in volume fraction of alumina in the composite. At an elevated temperature of 573 K the weakening effect of the composite at a given

TABLE II The variation in the values of constants of Equation 2 with the increase in temperature of the tensile tests

| Temperature (K) | Values of constants | | Correlation coefficient |
|---|---|---|---|
| | $m$ | ln $A$ | |
| 298 | −0.233 | −2.144 | 0.98 |
| 473 | −0.975 | −0.642 | 0.92 |
| 573 | −1.6 | 0.547 | 0.93 |

alumina content has been found to be more than that observed at 473 K or at ambient temperature up to ~ 7.0 to 8.0 vol % of alumina. $\alpha$ and the volume fraction of alumina, $V_{Al_2O_3}$, in the composite at 298, 473 and 573 K have been plotted on a log–log scale and the variations are almost linear as shown in Fig. 6. These curves can be approximately described by the equation

$$\ln \alpha = m \ln V_{Al_2O_3} + c \quad (2)$$

where, $m$ and $c$ are constants. The correlation coefficient of this linear fitting Equation 2 is more than 0.92 at all temperatures under investigation. Rewriting Equation 2 one gets

$$\alpha = A(V_{Al_2O_3})^m \quad (3)$$

when, $c = \ln A$. It is observed that the exponent $m$ of the composite is negative and increases with the increase in temperature as shown in Table II. The value of ln $A$ is negative at 298 and 473 K and it has been found to increase with the increase in temperature (see Table II).

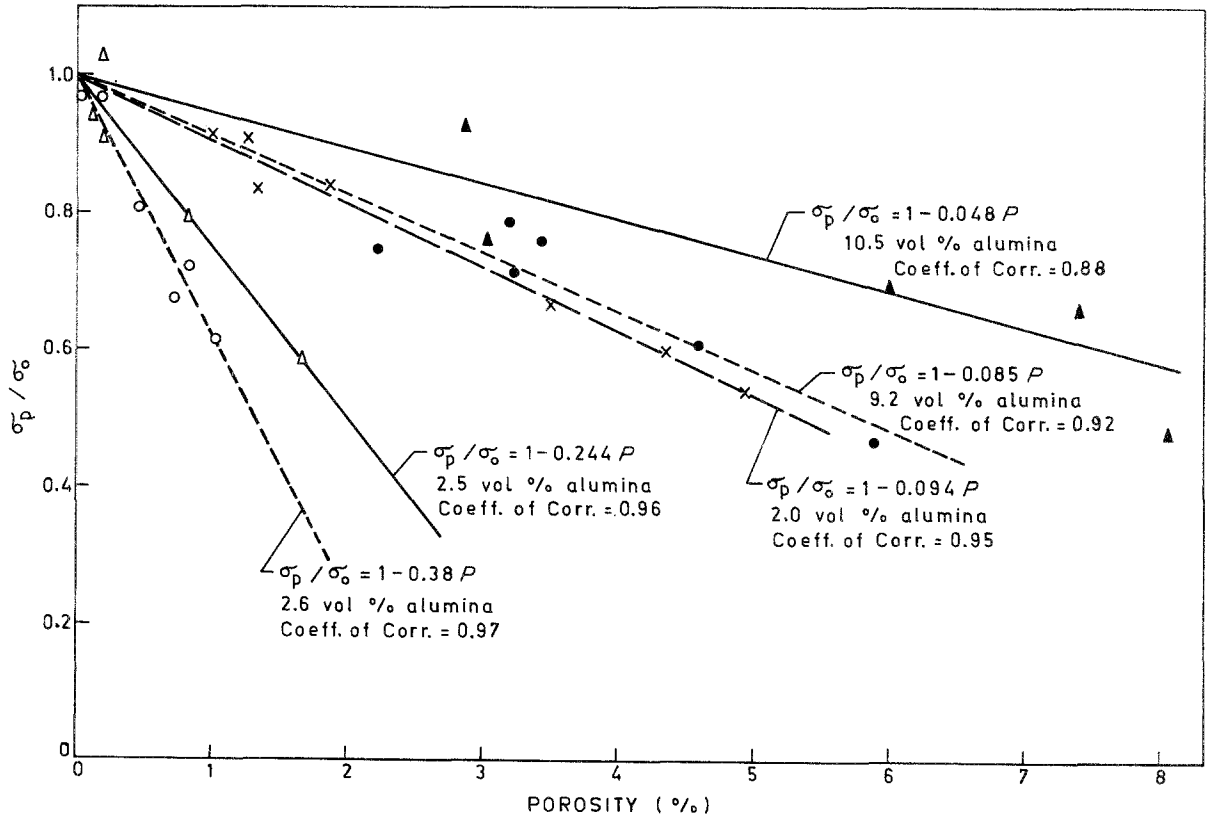


*Figure 4* Effect of porosity on the tensile strength ratio ($\sigma_p/\sigma_0$) in composites containing different amounts of alumina and tested at different temperatures. (– – –) 298 K, (——) 473 K, (- - -) 573 K. Vol % alumina: (○) ~2.6 ± 0.09, (●) ~9.2 ± 0.2, (△) ~2.5 ± 0.1, (▲) ~10.5 ± 0.4, (x) ~2.0 ± 0.1.

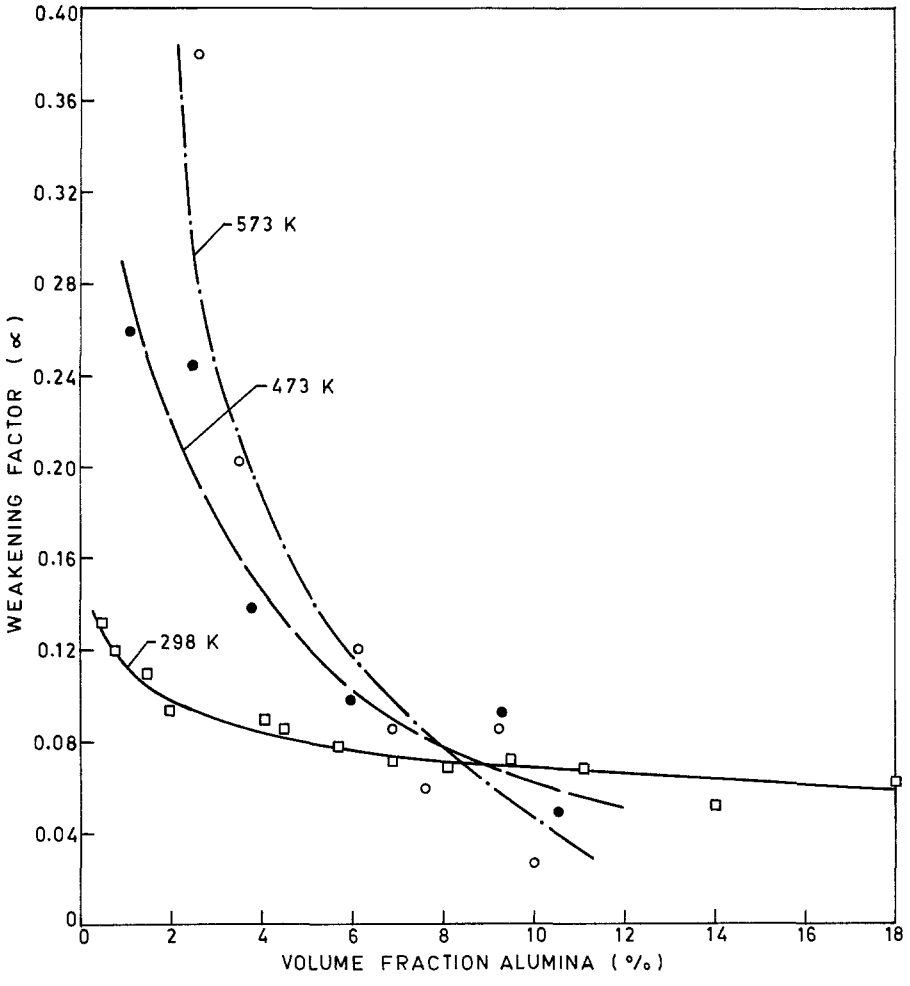


*Figure 5* Variation of weakening factor with alumina content of the composites at different temperatures. (□) 298 K, (●) 473 K, (○) 573 K.

The effect of particle content of the composite on its projected tensile strength at zero porosity, $\sigma_0$, at 298, 473 and 573 K are shown in Fig. 7. At both ambient and elevated temperatures it has been found that $\sigma_0$ decreases with an increase in volume fraction of alumina in the composite. For a given alumina content $\sigma_0$ has been found to be higher at lower temperatures compared to that observed at 573 K but it reduces drastically beyond ~9.0 to 9.5 vol % alumina at elevated temperatures. It is interesting to note that the

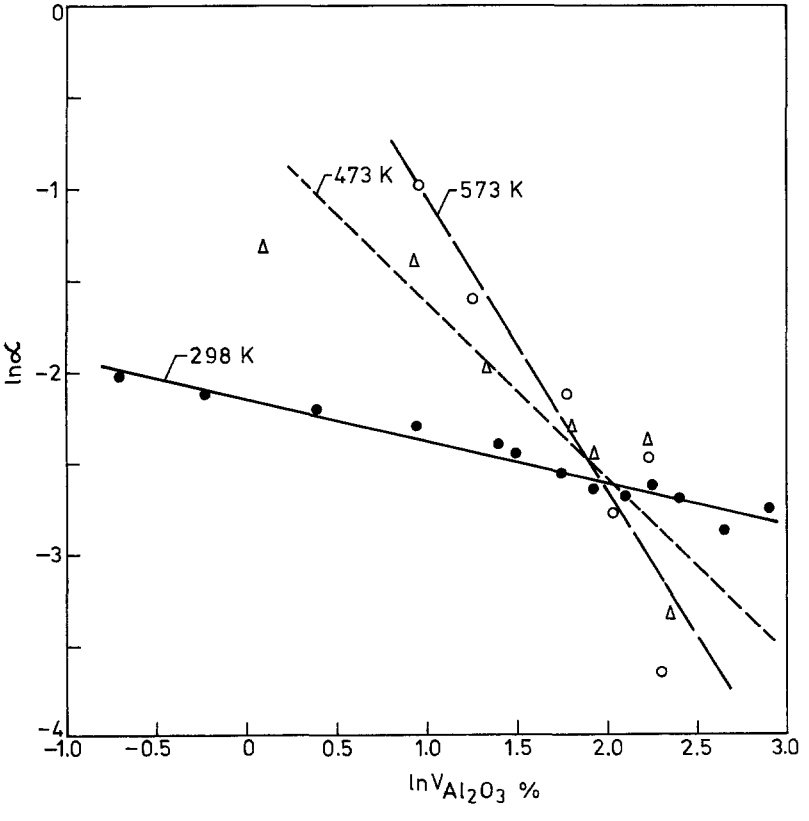


*Figure 6* Variation of ln α with ln $V_{Al_2O_3}$(%) of composites at different temperatures. (●) 298 K, (△) 473 K, (○) 573 K.

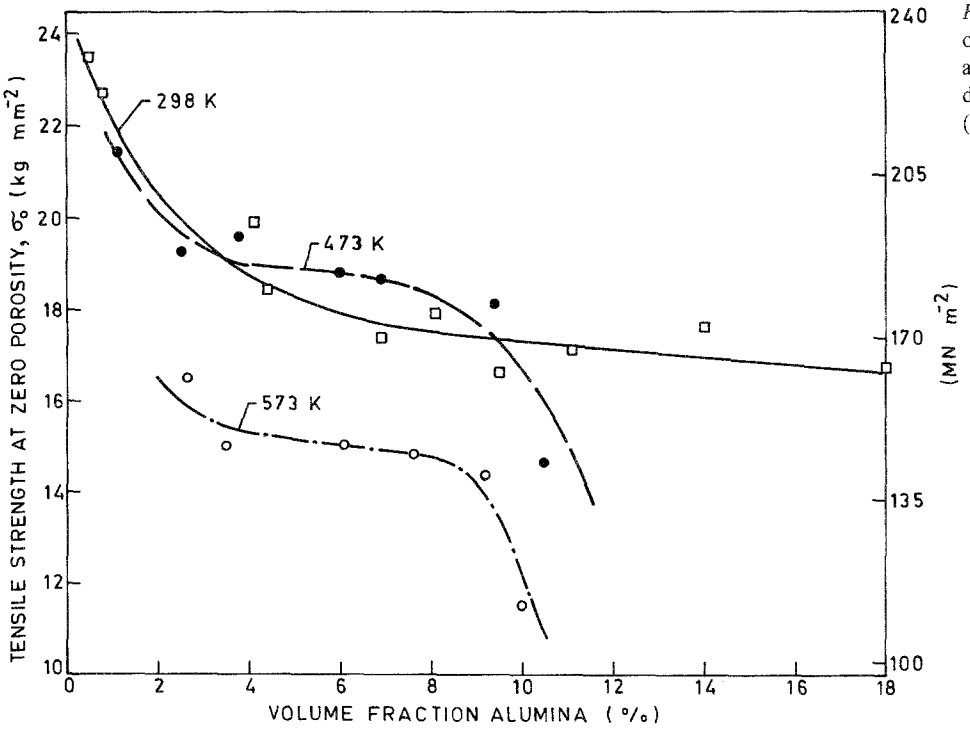


*Figure 7* Effect of particle content on the projected tensile strength at zero porosity for composites at different temperatures. (□) 298 K, (●) 473 K, (○) 573 K.

extent of reduction in $\sigma_0$ with temperature is quite small upto 473 K for an alumina content of $< 4.0$ vol % and between $\sim 4.0$ to 9.0 vol.% of alumina the composite shows the higher value of $\sigma_0$ at 473 K than that observed even at ambient temperature of 298 K.

Fig. 8 depicts the variation of $\alpha$ with the temperature of testing for composites having different extent of alumina varying from $\sim 2.6$ vol % to $\sim 10.3$ vol %. At alumina level between $\sim 2.6$ to $\sim 9.3$ vol.% $\alpha$ has been found to increase with an increase in temperature. But the weakening factor, $\alpha$, becomes relatively insensitive to temperature as the alumina content is increased. Beyond $\sim 10.3$ vol %

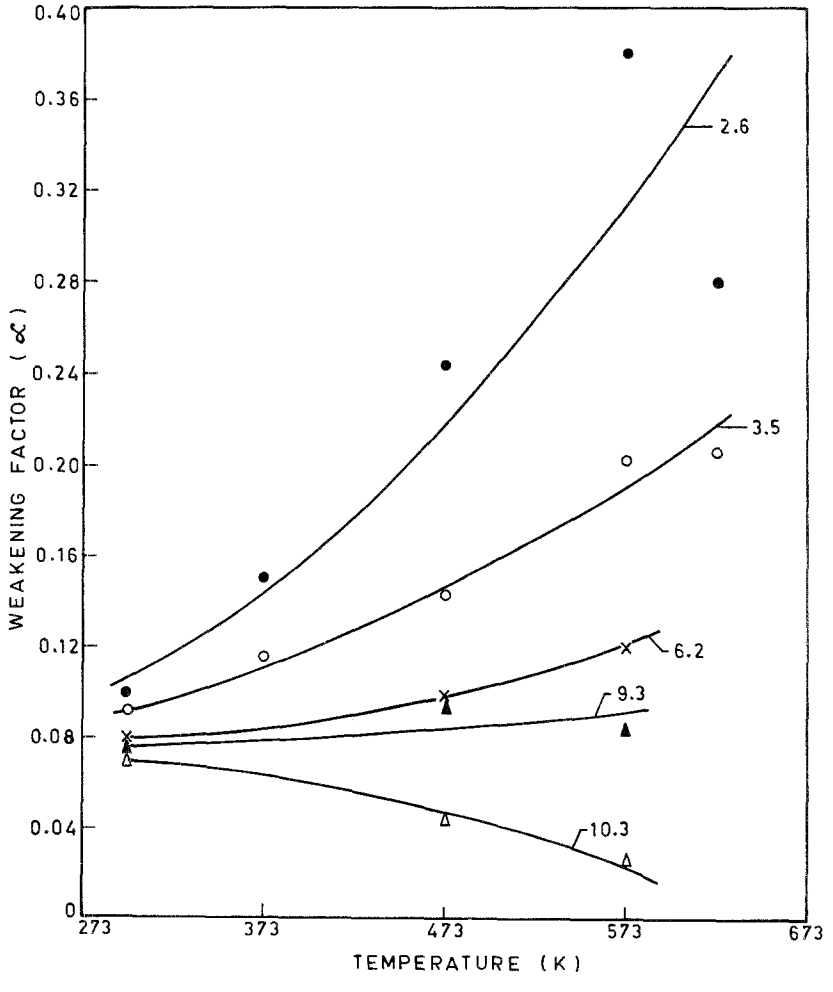


*Figure 8* Variation of weakening factor with temperature for composites containing given level of alumina particles. Vol % alumina: (●) $\sim 2.6 \pm 0.09$, (○) $\sim 3.5 \pm 0.14$, (x) $\sim 6.2 \pm 0.16$, (▲) $\sim 9.3 \pm 0.2$, (△) $\sim 10.3 \pm 0.41$.

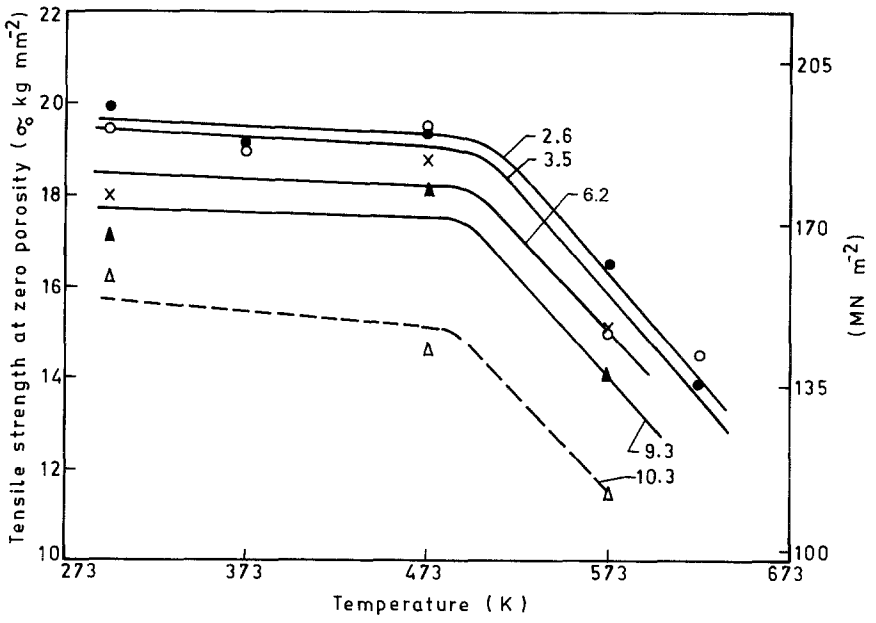


*Figure 9* Effect of temperature on the projected tensile strength at zero porosity for composites with given level of alumina particles. Vol % alumina: (●) ~2.6 ± 0.09, (○) ~3.5 ± 0.14, (x) ~6.2 ± 0.16, (▲) ~9.3 ± 0.2, (△) ~10.3 ± 0.41.

alumina the nature of variation of $\alpha$ with temperature is reversed and it reduces with an increase in temperature.

The corresponding values of $\sigma_0$ shows a minor decrease with an increase in temperature up to 473 K followed by a rapid drop with a further increase in temperature as it has been commented earlier and further evident in Fig. 9. At any given temperature the values of $\sigma_0$ have been found to be higher at lower alumina content. The variation in ultimate tensile strength of composites having a given alumina content with an increase in temperature has been shown in Fig. 10. The figure shows a similar trend to that observed in Fig. 9.

The effect of temperature on the engineering stress–strain behaviour of the composite having alumina and porosity content of ~2.4 and ~0.14 vol %, respectively has been shown in Fig. 11. The figure shows that with the increase of temperature from the ambient temperature to 623 K the failure of the composite takes place at a lower stress level but the fracture strain, in general, is enhanced. Upto a temperature of 473 K a continuous increase of strain with the rise of stress is observed until fracture. However, at temperatures of 573 and 623 K, the composite deforms continuously without any appreciable change in stress beyond a certain level of strain which reduces with an increase in temperature.

The variation in average fracture strain ($e_f$) with an increase in temperature from 373 to 623 K has been given in Table III for composites having different amounts of alumina at a given volume fraction of porosity. The table shows that at the lower levels of alumina content below ~8.98 vol % the fracture strain of the composites increases with an increase in temperature. However, in the case of higher alumina content beyond the amount mentioned above the fracture strain of the composite decreases with the increase in its temperature.

Fig. 12 shows the relation between fracture strain $e_f$

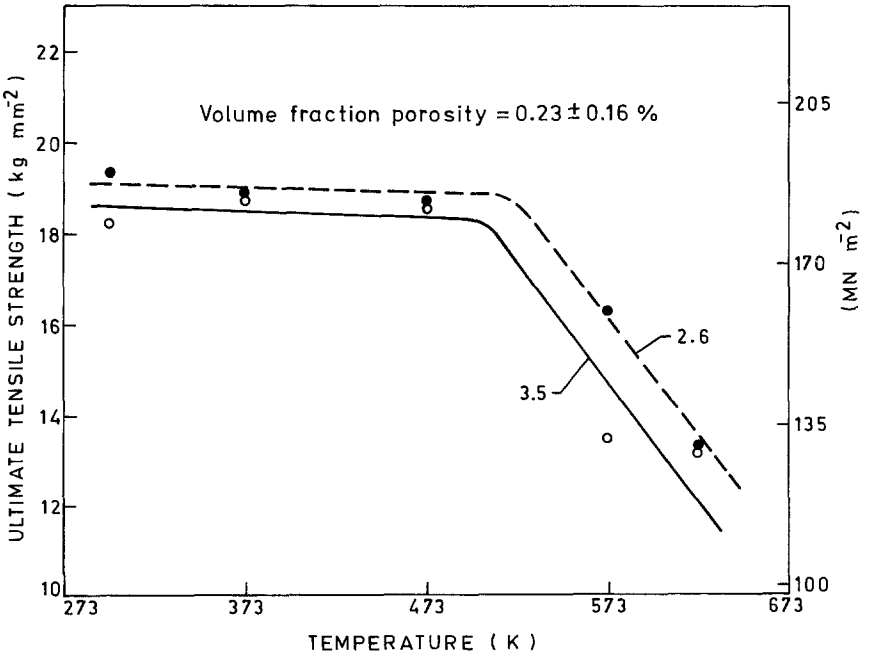


*Figure 10* Effect of temperature on the ultimate tensile strength of composite with given alumina content. Volume fraction porosity = 0.23 ± 0.16%. Volume fraction alumina (●) ~2.6 ± 0.17%, (○) ~3.5 ± 0.25%.

TABLE III Variation in average fracture strain ($e_f$) with temperature in different composites

| Volume fraction porosity (%) | Volume fraction alumina (%) | Average fracture strain ($e_f$) at elevated temperature | | | |
|---|---|---|---|---|---|
| | | 373 K | 473 K | 573 K | 623 K |
| 0.117 ± 0.08 | 2.64 ± 0.17 | 0.106 | 0.117 | 0.131 | 0.147 |
| 0.47 ± 0.08 | 2.51 ± 0.19 | 0.08 | 0.09 | – | 0.097 |
| | 3.59 ± 0.29 | 0.09 | 0.122 | – | 0.164 |
| 1.43 ± 0.26 | 3.69 ± 0.29 | 0.082 | – | – | 0.107 |
| | 6.07 ± 0.17 | | 0.048 | 0.064 | – |
| | 3.35 ± 0.3 | – | 0.04 | 0.058 | 0.085 |
| 3.17 ± 0.48 | 8.98 ± 0.39 | – | 0.0475 | 0.047 | – |
| | 10.33 ± 0.28 | – | 0.049 | 0.036 | – |
| 7.26 ± 1.5 | 9.97 ± 0.68 | – | 0.0396 | 0.032 | 0.026 |

and the reciprocal of the percentage of porosity, $P^{-1}$, as observed at various temperatures in a composite containing ~9.4 vol% alumina. Least-squares straight lines have been fitted to the experimental points with a correlation coefficient of 0.89 and more. the lines at elevated temperatures have been forced The lines at elevated temperatures have been forced origin (0, 0). The nature of the curves may be approximately described by the equation

$$e_f = m'/P + c' \quad (4)$$

The values obtained for constants $m'$ and $c'$ in Equation 4 are given in Table IV. At a given porosity level the $e_f$ of a composite containing ~9.4 vol% alumina has been found to decrease with an increase in temperature.

The longitudinal section of the tensile specimens having ~3.6 vol% alumina and ~0.45 vol% of porosity, and tested at 373, 473 and 623 K have been observed under a scanning electron microscope to reveal the preferred sites for nucleation of voids along the boundary of the primary particles in the matrix as prevalent near the fracture surface shown in Figs 13a, b and c, respectively. The figures show that before fracture the extent of growth and linkage of voids become extensive at higher temperature of 623 K (Fig. 13c). The fractograph of a composite having 10.0 vol% alumina and 3.0 vol% of porosity tested under tension at 473 K is given in Fig. 14 to show the propagation of a crack initiated from a void created by particle–matrix debonding. The composites having about 9.8 vol% alumina and 2.9 vol% porosity have been tested under tension at ambient and elevated temperatures of 298, 473 and 573 K and the fracture characteristics are shown in Figs 15a, b and c, respectively. Fig. 15a reveals that at 298 K the failure of the composite has taken place by a mixed mode of ductile and clevage fracture. However, the fractographs (Figs 15b and c) of the composites failed at elevated temperatures of 473 and 573 K show that the size of the dimples become comparatively larger at higher temperature (573 K) than that observed at the lower temperature of 473 K. It is also interesting to note that a number of considerably smaller dimples (marked by arrows) along with the larger one are also present in the fractured surface of the composite tested at 573 K as shown in Fig. 15b.

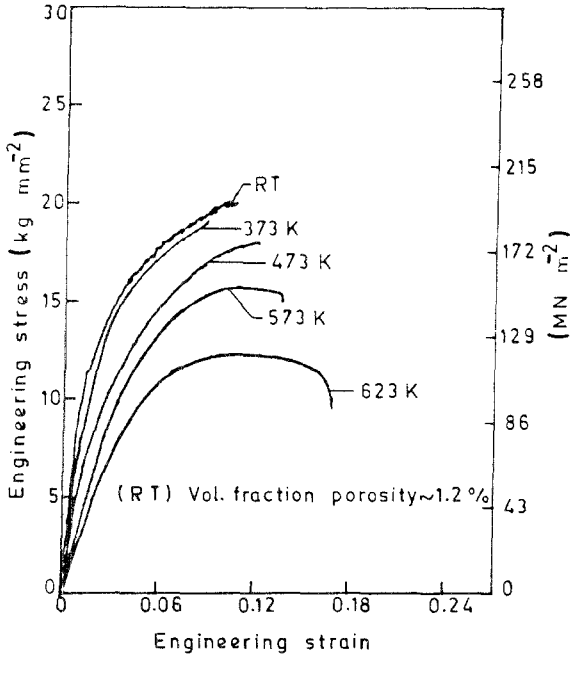


*Figure 11* Effect of temperature on engineering stress–strain curve of composites with given alumina content. Volume fraction: $Al_2O_3$ ~ 2.4%, porosity ~0.14%.

The optical micrographs of the longitudinal section near the fractured surface of the tensile specimens containing ~3.17 vol% alumina, ~0.2 vol% porosity and tested at 473, 573 and 623 K are shown in Figs 16a, b and c, respectively. Fig. 16a shows the presence of as-cast primary particles in the matrix even after it has been held at 473 K during testing. However, in the microstructures of the specimens tested at 573 and 623 K (Figs 16b and c), respectively a large number of newly formed fine grains have been found to exist surrounding the primary α and alumina particles.

TABLE IV The variation in the values of constants of Equation 4 with an increase in test temperature

| Temperature (K) | Values of constants | | Correlation coefficient |
|---|---|---|---|
| | $m'$ | $c'$ | |
| 298 | 0.2 | −0.008 | 0.94 |
| 473 | 0.17 | −0.004 | 0.89 |
| 573 | 0.14 | −0.003 | 0.91 |

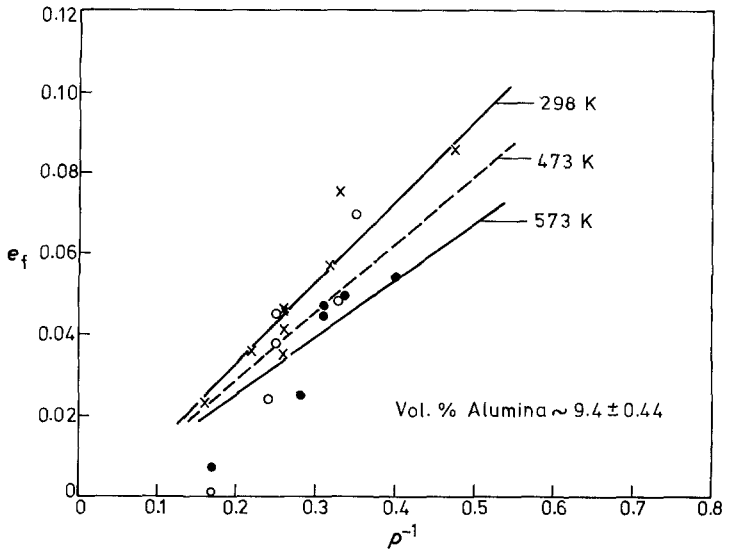


*Figure 12* Effect of inverse volume percentage porosity on engineering fracture strain of composites tested at different temperatures. Vol % alumina ~9.4 ± 044, (x) 298 K, (○) 473 K, (●) 573 K.

Fig. 16c also reveals that the newly formed grains have become coarser at 623 K in comparison to that observed at 573 K as shown in Fig. 16b.

## 4. Discussion

The porosity content of a compocast composite is directly correlated with the inhomogeneity in particle distribution. Microscopic observations reveal that well separated particles do not generally have a void at the interface (Fig. 2). However, a cluster of particles (Fig. 3) often has voids because during the stirring of the slurry in a vortex method of fabrication of cast composites the air bubbles sucked inside the slurry through the vortex may be trapped in the cluster of particles in case of a certain bubbles–particle configuration. It has been observed earlier [3] that in the compocast composites a higher level of porosity results along with an increased tendency of particle clustering and these clusters with voids create inhomogeneous regions of weakness.

The linear variation of the ratio of ultimate tensile strength at porosity $P$ to that at zero porosity, $\sigma_p/\sigma_0$, with volume fraction of porosity as shown in Fig. 4 confirms the applicability of the model Equation 1 for estimating the contribution of porosity on the elevated temperature tensile strength of the composite. At a given close range of alumina content (2.0 to 2.6 vol %) the increase in weakening factor, $\alpha$, with an increase in test temperature as shown in Fig. 4 is attributed to enhanced elongation resulting in larger debonding at the end of uniform elongation. Also, the pores are more elongated resulting in increased coalescence.

The damaging effect of porosity to the tensile load bearing capacity has been observed [2] to take place by the development of a surrounding non-uniform stress field and its magnitude is governed by the mechanical

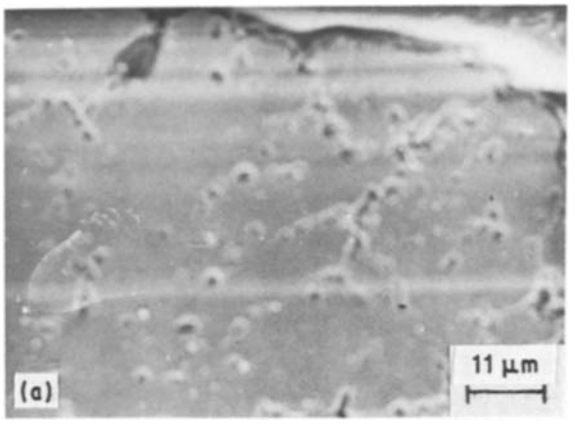


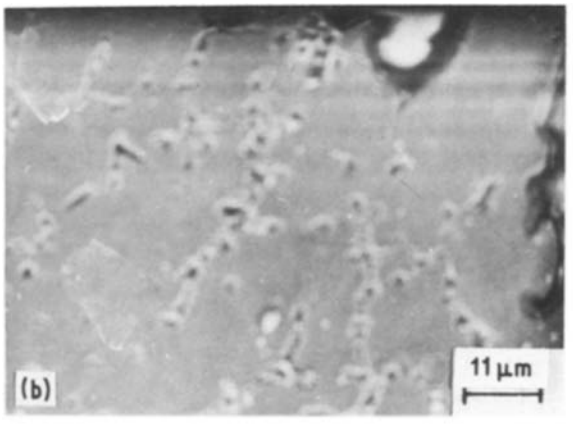


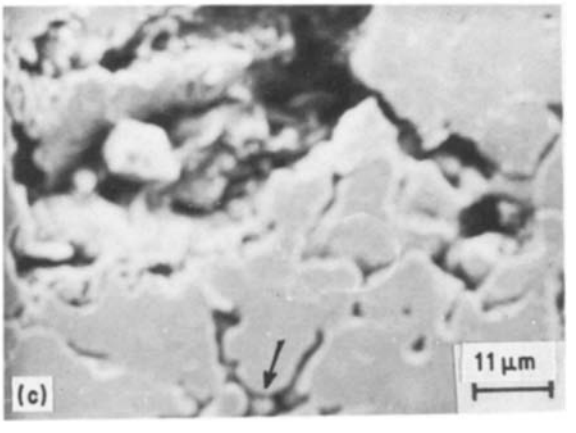


*Figure 13* Scanning electron micrographs showing the matrix near the fractured surface of composites tested at different temperatures. (a) a 373 K, (b) at 473 K and (c) at 623 K.

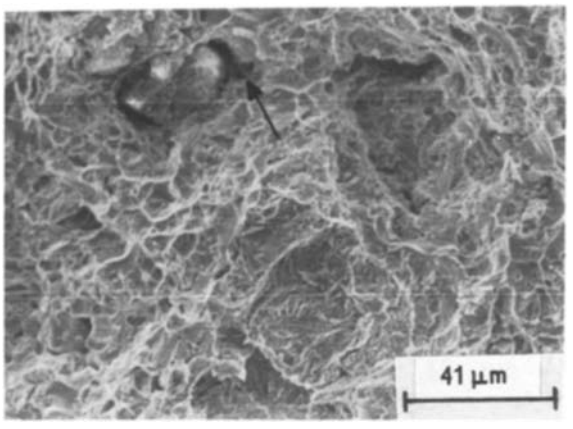


*Figure 14* Fractograph showing the path of propagation of a crack initiated from a void created by particle–matrix debonding at 473 K.

characteristics of the matrix. The distribution of stress is controlled by the magnitude of flow stress and the dispersion of pores in the matrix. The presence of particles in a composite helps to reduce the elongation to result in a less deleterious effect of porosity [3]. Also, a lower total elongation will cause a reduction in the extent of particle–matrix debonding. However, at elevated temperatures a reduction in flow stress results in a substantial plastic flow even around the particles giving rise to enhanced debonding. Thus, the particles have a contradictory role of reinforcing the weakening effect of porosity at larger elongations and restraining the weakening effect by reducing the elongation. Below ~9.0 vol % alumina the particles help weakening at elevated temperature but beyond this level the dominating influence comes from its role in the elongation to reduce the influence of porosity as shown in Figs 5 and 8. It is further evident from Fig. 12 that a lower fracture strain is observed at elevated temperatures for a composite containing alumina in excess of ~9.0 vol %.

The power law relationship between $\alpha$ and $V_{Al_2O_3}$ given in Fig. 6 has a correlation coefficient in the range of 0.92 to 0.98 (Table II) and it further confirms the trends of variation in $\alpha$ with a change in temperature as observed in the composites containing a given level of alumina lying below and above ~9.0 vol %.

The nucleation of voids at the particle–matrix interface and its growth leading to the formation of a crack has been shown in Fig. 14 and it causes a progressive deterioration in load bearing capacity in a composite. At higher temperatures due to a lower flow stress in a composite with ~2.4 vol % $Al_2O_3$ an extensive plastic flow at the tip of crack results in blunting the crack. Thus coalescence of voids is delayed as reflected in the observed absence of serrations in the tensile stress–strain curve with the rise of temperature shown in Fig. 11.

The projected ultimate tensile strength (UTS) at zero porosity, $\sigma_0$, of the composites has been found to reduce slowly with an increase in alumina content upto about 9.0 vol % at higher temperatures of 473 and 573 K than that observed at 298 K. As such in the range of alumina content between 4.0 and ~9.0 vol % $\sigma_0$ of the composites show a comparatively higher value at 473 K than those obtained when they are tested at 298 K as shown in Fig. 7. However, at elevated temperatures of 473 and 573 K the abrupt lowering of $\sigma_0$ with an increase in alumina content beyond ~9.0 vol % indicates an early debonding of particles.

The increase in temperature reduces the strain hardening exponent due to thermally activated deformation leading to flattening-out [4] of the stress–strain curve (Fig. 11) and gives rise to an improvement in % elongation of the composites having less than ~9.0 vol % $Al_2O_3$ as revealed in the fractographs presented in Fig. 15 wherein it has been

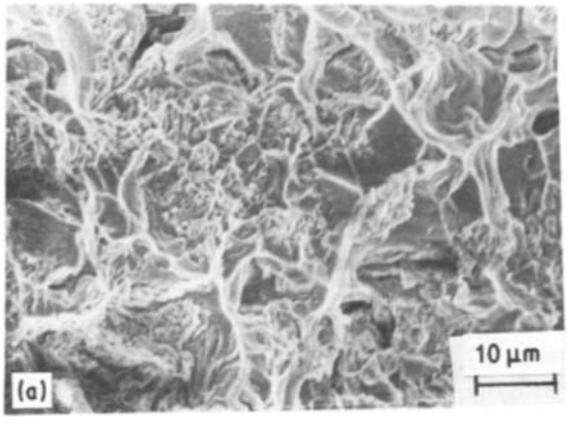


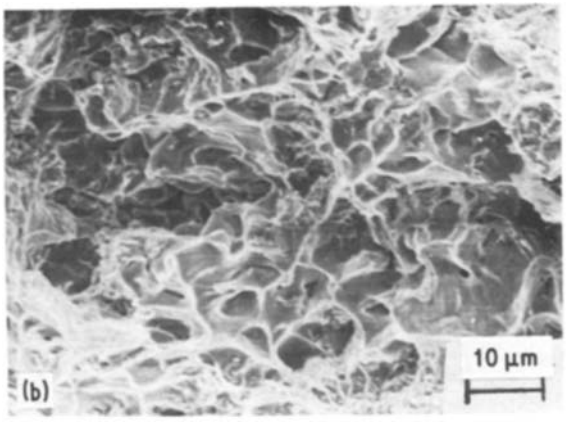


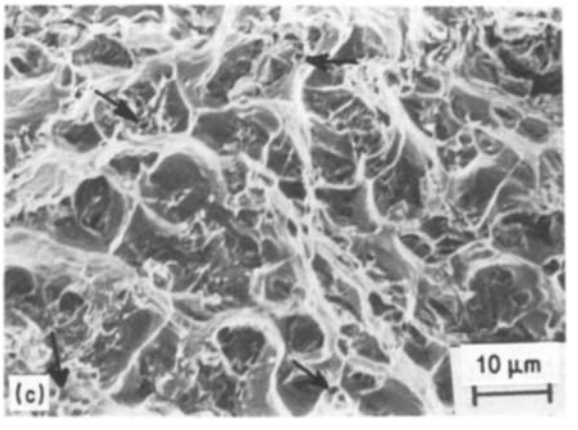


*Figure 15* Fractographs of the composites showing an increasing extent of ductile fracture with temperature and a number of fine dimples (arrow marked) appearing when tested at 573 K. (a) at 298 K, (b) at 473 K and (c) at 573 K.

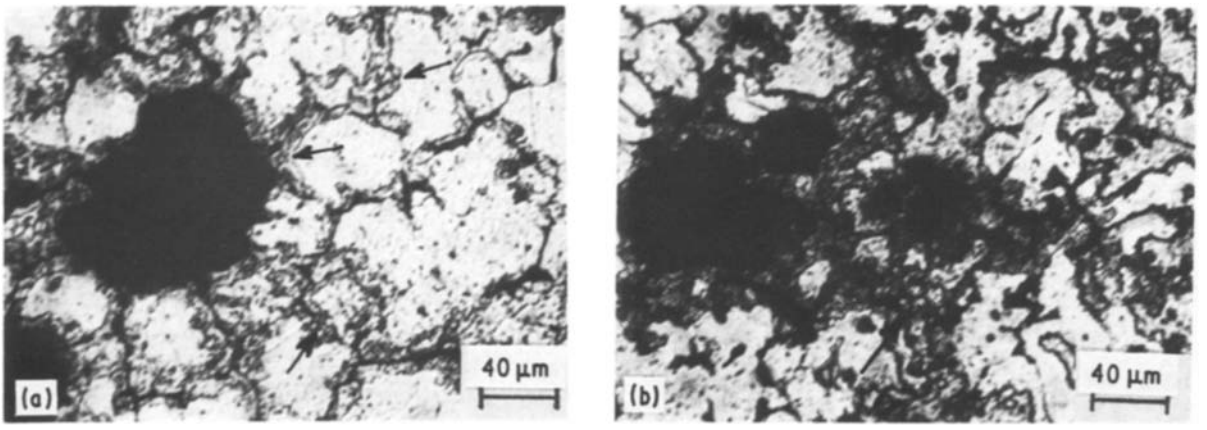


*Figure 16* Optical micrographs of the matrix near the fractured surface of the composites showing the recrystallization and grain growth (arrow marked) when tested at (a) 573 K and (b) 623 K, respectively.

observed that from 473 K the fracture is characterized by the formation of dimples (Fig. 15b) whose size have increased (Fig. 15c) with the rise of temperature to 573 K. It is interesting to note that at a temperature above 573 K the flattening is observed to an extent that there is an almost flat region in the engineering stress–strain curve (Fig. 11). This may be attributed to the occurrence of recrystallization near the fractured surface observed as newly formed fine grains [5] revealed in the micrograph presented in Fig. 16 and subsequent grain growth at 623 K as shown in Fig. 16c. The presence of a significant amount of fine dimples in the fractograph (Fig. 15c) have possibly resulted from the fracture of recrystallized grains in the composite formed at 573 K. An increase in test temperature also enhances the grain-boundary sliding giving rise to the formation of voids at the grain boundary at a lower stress. This void formation is further favoured in presence of second phase particles at the grain boundary [6] and initiate grain boundary cracks by the growth and coalescence of voids under a joint action of vacancy diffusion and grain boundary sliding. As a result there is an increase in the extent of nucleation and growth of voids leading to the generation of cracks with the rise in test temperature as revealed in the microstructures presented in Figs 13a, b and c of the matrix near the fractured surface of a composite having $\sim 3.6$ vol % alumina tested at temperatures 373, 473 and 623 K, respectively. Further, the zones having recrystallization and grain growth at higher temperatures will have a considerably lower strength but there will be no grain-boundary shearing in it. These factors taken together may have caused a drastic fall of $\sigma_0$ (Fig. 9) with the rise of temperature to beyond $\sim 500$ K. There is a similarity in the trend of variation in the ultimate tensile strength (Fig. 10) and the variation of $\sigma_0$ (Fig. 9) with the rise in temperature of testing composites with different levels of alumina content.

The recrystallization and grain-boundary migration accommodates the stress concentration introduced by straining near grain boundaries and improves the ductility of the composites with an increase in its temperature giving rise to a higher fracture strain ($e_f$) as shown in Table III. However, this variation of $e_f$ with temperature is particularly marked at lower alumina contents ($< 8.98$ vol %) but in composites with high amounts of alumina an opposite trend of variation of $e_f$ with the rise in temperature is observed due to the resistance of a larger number of particles to plastic flow as discussed above.

## References

1. P. K. GHOSH, S. RAY and P. K. ROHATGI, *Trans. Jpn Inst. Met.* **25** (6) (1984) 440.
2. P. K. GHOSH, P. R. PRASAD and S. RAY, *Z. Metallkde.* **75** December (1984) 934.
3. P. K. GHOSH, S. RAY, *J. Mater. Sci.* **21** (5) (1986) 1667.
4. G. E. DIETER, "Mechanical Metallurgy", 2nd edn (McGraw Hill, Kogakusha, 1976) p. 335.
5. T. TAKASUGI and O. IZUMI, *Acta Metall.* **33** (1) (1985) 39.
6. G. E. DIETER, "Mechanical Metallurgy", 2nd edn (McGraw Hill, Kogakusha, 1976) p. 241.

*Received 6 January*
*and accepted 4 March 1987*